Journal of Solid State Chemistry **157,** 144–148 (2001)
doi:10.1006/jssc.2000.9066, available online at http://www.idealibrary.com on IDEAL®

Electrical and Magnetic Properties of New Mixed Transition Metal Sulfides $BaKCu_3MS_4$ (M = Mn, Co, Ni)

M. Mouallem-Bahout,[1] O. Peña, and C. Carel

Laboratoire CSIM, UMR du CNRS 6511, Université de Rennes 1, CS 74205, 35042 Rennes Cedex, France

and

A. Ouammou

Laboratoire Matériaux et Protection de l'Environnement, Département de Chimie, Faculté des Sciences Dhar Mehraz, Université Sidi Mohamed Ben Abdellah, B.P. 1796 Atlas, Fès, Morocco

Received July 7, 2000; in revised form December 4, 2000; accepted December 8, 2000

New transition metal sulfides $BaKCu_3MS_4$ (M = Mn, Co, Ni) were prepared from $BaCO_3$, K_2CO_3, and the corresponding transition metal oxides by CS_2/Ar sulfurization. The materials are based on a common structural pattern consisting of 2-D arrangements of MS_4 tetrahedra linked by edges, crystallizing in the tetragonal $ThCr_2Si_2$-type structure in space group $I4/mmm$. Electrical resistivity measurements show that the new phases are semiconducting. The temperature dependence of magnetic susceptibility shows different behaviors depending on the substituting transition element: the data for $BaKCu_3MnS_4$ can be fitted to the Curie–Weiss equation ($\mu_{eff} = 2.50\ \mu_B$ per manganese ion) while magnetic ordering occurs for $BaKCu_3CoS_4$ ($T_N \sim 12$ K). $BaKCu_3NiS_4$ exhibits temperature–independent paramagnetic behavior. © 2001 Academic Press

Key Words: **quaternary sulfides; layered structure; magnetic interactions; Néel temperature.**

1. INTRODUCTION

Transition metal intercalates of sulfur-based compounds have attracted growing interest in recent years because of their similarity to the high-temperature copper oxide superconductors (1) and their potential applications in important technologies such as cathodes in electrochemical cells (2, 3). The mixed transition metal sulfides with the formula $ACu_{2x-1}MS_{2x}$ (A = K, Rb, Cs; M = Fe, Mn; x = 1, 2) that we have been studying recently belong to this group of compounds with the tetragonal $ThCr_2Si_2$-type structure (4). In our continuing exploration of new solid-state copper sulfides, we report, in this paper, the results of a partial substitution of both Ba and Cu within the Ba–Cu–S system. This led to the isolation of new copper-based sulfides materials, $BaKCu_{3.5}Fe_{0.5}S_4$ (5), $BaKCu_3ZnS_4$ (6), and $BaKCu_3MS_4$ (M = Mn, Co, Ni). The structural characterization and electrical and magnetic properties of those latter compounds are discussed.

[1] To whom correspondence should be addressed. E-mail: mona.bahout@univ-rennes1.fr.

2. EXPERIMENTAL SECTION

2.1. Synthesis

The procedure to obtain copper-based sulfides involves sulfurization in a stream of CS_2 carried by Ar gas. The starting materials $BaCO_3$, K_2CO_3, CuO, and the corresponding transition metal oxide (MnO_2,CoO, or NiO) were mixed in an agate mortar in a stoichiometric ratio. The powder mixture was then placed in an alumina boat and heated in a tube furnace in a CS_2/Ar atmosphere at any temperature in the range 850°C–950°C, whatever the phase may be. After ~7 hours, the furnace was shut off and allowed to cool in a stream of dried argon. All of the samples are dark gray and air stable. Their purity was examined by powder X-ray diffraction analysis.

2.2. Physical Measurements

Quantitative microprobe analyses were carried out with a JEOL JSM-6400 scanning electron microscope (SEM) equipped with an energy dispersive spectroscopy (EDS) detector. The analyses were performed on a large number of different surface points on each grain in order to confirm the homogeneity of the products and the composition of the samples (Table 1). The powder X-ray diffraction (PXD) data were collected with a Philips computer-controlled powder diffractometer operating at 35 kV, 35 mA. CuK_α radiation

0022-4596/01 $35.00

TABLE 1
Results of the Elemental Analysis of $BaKCu_3MS_4$ (M = Mn, Co, Ni) (Accuracy±5%)

Composition	Ba (at.%)	K (at.%)	Cu (at.%)	M (at.%)	S (at.%)
		$BaKCu_3MnS_4$			
Experimental	9.79	11.17	29.27	9.39	40.50
Calculated	10.00	10.00	30.00	10.00	40.00
		$BaKCu_3CoS_4$			
Experimental	9.81	12.05	28.62	9.98	39.58
Calculated	10.00	10.00	30.00	10.00	40.00
		$BaKCu_3NiS_4$			
Experimental	9.80	12.05	28.62	9.98	39.59
Calculated	10.00	10.00	30.00	10.00	40.00

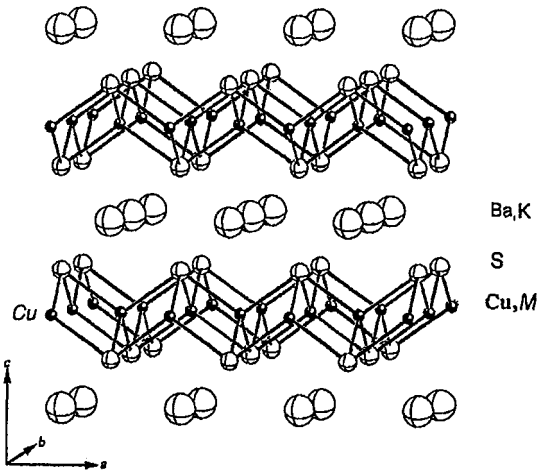

FIG. 1. Structural arrangement for $BaKCu_3MS_4$ (M = Mn, Co, Ni).

was used in the 2Θ range 10°–60° for the purpose of identification and phase purity determination and in the least-squares refinement of the unit cell parameters. Transport measurements were carried out on sintered pellets (~500°C in a CS_2 atmosphere) by a standard four-probe technique with a closed-cycle cryostat (TBT, Air Liquide) from room temperature to ~ 75 K for the nickel and manganese compounds and to $T \sim 120$ K for the cobalt phase. Below 120 K, the resistivity of the latter compound was too high to be detected with our setup. Ohmic contacts were made by attaching gold threads to four spots of conducting silver paste on the side of a brick-shaped polycrystalline pellet. Magnetic susceptibility measurements were performed with a SQUID magnetometer (SHE VTS-906) on polycrystalline materials. Field dependence studies were always performed first, and a suitable magnetic field was chosen from the linear region for temperature dependence measurements.

3. RESULTS AND DISCUSSION

3.1. Structure Determination

All of the materials were examined by X-ray powder diffraction for the purpose of identification and phase purity determination. The powder patterns could be indexed in a tetragonal cell, with the well-known layered $ThCr_2Si_2$ structure (Fig. 1). It consists of a 2-D arrangement of MS_4 tetrahedra sharing all edges, extended in the *ab* plane and pointing up and down with their apices. The mixed transition elements Cu and M (M = Mn, Co, or Ni) occupy the centers of the tetrahedra either in a random way or in a preferential order. Owing to the small difference in scattering factors between Cu and M, any crystallographic ordering on the tetrahedral site may evade detection by means of classical X-ray powder diffraction. However, the most probable effect is that the transition element M would randomly occupy the copper site.

The Ba/K ions, eight-coordinated by S ions, are located between the $(Cu_{1.5}M_{0.5}S_2)^{1.5-}$ layers. A statistical disorder of K^+ and Ba^{2+} on the same site might probably occur owing to similar ionic radii (1.78 Å and 1.74 Å for K^+ and Ba^{2+}, respectively). In Table 2 are given the least-squares refined unit cell parameters of the compounds studied in this work, along with those of similar phases reported previously. A comparison of the d spacings is given in Table 3.

3.2. Transport Properties

The mixed alkali/alkaline earth-based phase $Ba_{0.80}K_{0.20}Cu_2S_2$ exhibits a metallic behavior which contrasts with the semiconducting behavior of the parent compound $BaCu_2S_2$. The difference has been attributed to the presence of a certain amount of Cu^{2+} (d^9) in $Ba_{0.80}K_{0.20}Cu_2S_2$ while copper ions are monovalent Cu^+ (d^{10}) in $BaCu_2S_2$ (7, 8). We decided to investigate structurally related systems in which a larger concentration of copper ions has been replaced by nonisoelectronic transition elements. Figure 2 shows that the resistivity of $BaKCu_3MS_4$ compounds increases with

TABLE 2
Unit Cell Parameters for $BaKCu_3MS_4$ (M = Mn, Co, Ni) Refined from Powder X-Ray Patterns

Compound	a (Å)	c (Å)
$BaKCu_3MnS_4$	3.920(2)	12.987(4)
$BaKCu_3CoS_4$	3.892(3)	12.869(2)
$BaKCu_3NiS_4$	3.874(2)	12.775(4)
$BaKCu_3ZnS_4$ (6)	3.903(3)	12.964(2)
$Ba_{0.80}K_{0.20}Cu_2S_2$(8)	3.900(1)	12.686(2)
$BaCu_2S_2$ (7)	3.908(1)	12.656(2)

Note. The estimated standard deviation is given in parentheses.

TABLE 3
Powder X-Ray Diffraction Data of $BaKCu_3MS_4$ (M = Mn, Co, Ni), Space Group $I4/mmm$

			$BaKCu_3MnS_4$			$BaKCu_3CoS_4$			$BaKCu_3NiS_4$		
h	k	l	d_{calc}	d_{obs}	I/I_0	d_{calc}	d_{obs}	I/I_0	d_{calc}	d_{obs}	I/I_0
0	0	2	6.493	6.488	100	6.435	6.451	47	6.388	6.384	100
1	0	1	3.753	3.751	21	3.724	3.725	22	3.707	3.708	3
0	0	4	3.247	3.248	28	3.218	3.220	36	3.194	3.186	75
1	0	3	2.906	2.903	17	2.882	2.883	100	2.866	2.864	26
1	1	0	2.772	2.768	13	2.752	2.753	17	—	—	—
1	1	2	2.549	2.546	21	2.530	2.531	32	2.518	2.515	89
1	0	5	2.165	2.165	13	2.147	2.148	34	2.133	2.131	5
1	1	4	—	—	—	2.091	2.091	71	2.079	2.079	15
2	0	0	—	—	—	1.946	1.946	31	1.937	1.938	5
1	1	6	1.706	1.705	27	1.692	1.692	32	1.681	1.681	28
2	0	4	—	—	—	—	—	—	1.656	1.657	7
2	1	3	—	—	—	1.613	1.627	—	1.605	1.603	5
0	0	8	1.623	1.624	14	1.609	1.609	21	1.597	1.597	16

decreasing temperature, as usual for nonmetallic materials. Such semiconducting behavior, probably due to the presence of localized electrons in narrow bands, is expected since different ions are disordered on the same crystallographic site. Indeed, Brun *et al.* (9) and Berger *et al.* (10) found that replacement of one-fourth of the Cu atoms in $TlCu_2Se_2$ by Fe ions resulted in changing the properties from highly metallic to semiconducting behavior.

The semiconducting properties of $BaKCu_3MS_4$ compounds, which contrast with the results of Hückel tight-binding calculations (11), show that such a model is not sufficiently accurate to predict metallic or insulating behavior in the present case. The disagreement between the electronic structure and the experimental behavior suggests that $BaKCu_3MS_4$ materials are Mott insulators.

3.3. Magnetic Susceptibility Measurements

The temperature dependence of the magnetic susceptibility χ for the new phases is presented in Figs. 3 and 4. The magnetic parameters obtained from these plots are summarized in Table 4.

Figure 3 suggests Curie-type behavior down to 2 K for $BaKCu_3MnS_4$ with an effective magnetic moment of 2.50 μ_B. This behavior contrasts with that of the structurally related phases $ACuMnS_2$ (A = K, Rb, Cs) where antiferromagnetic exchange in isolated manganese clusters has been suggested (12). That $BaKCu_3MnS_4$ does not exhibit long-range coupling is consistent with its lower concentration of manganese ions compared to that of the $ACuMnS_2$ compounds; the mean Mn–Mn distance in $BaKCu_3MnS_4$ is

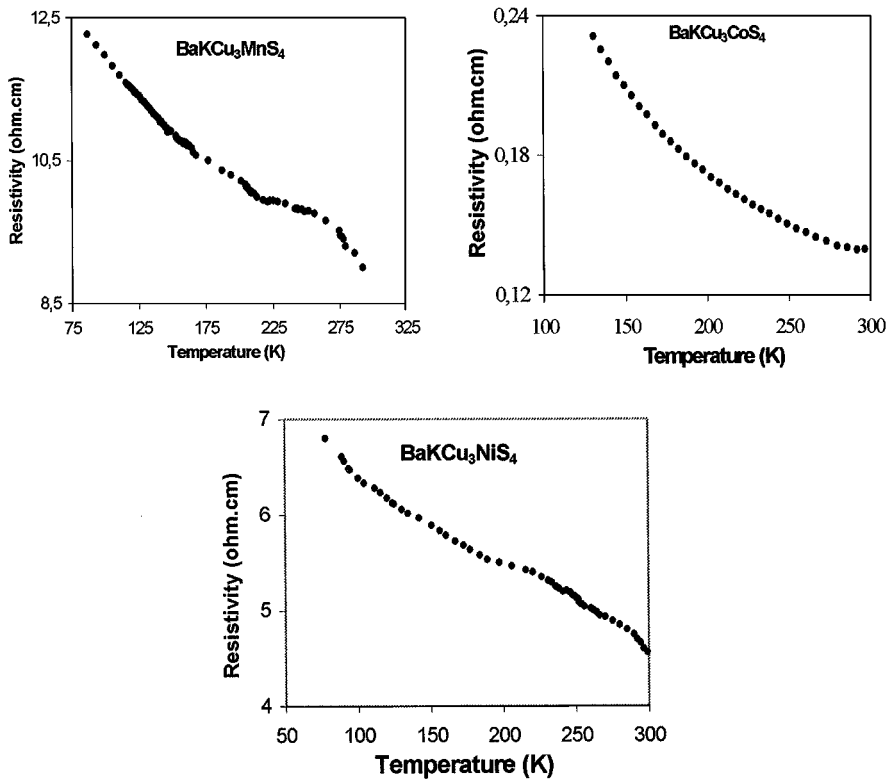

FIG. 2. Electrical resistivity of $BaKCu_3MnS_4$, $BaKCu_3CoS_4$, and $BaKCu_3NiS_4$ as a function of temperature.

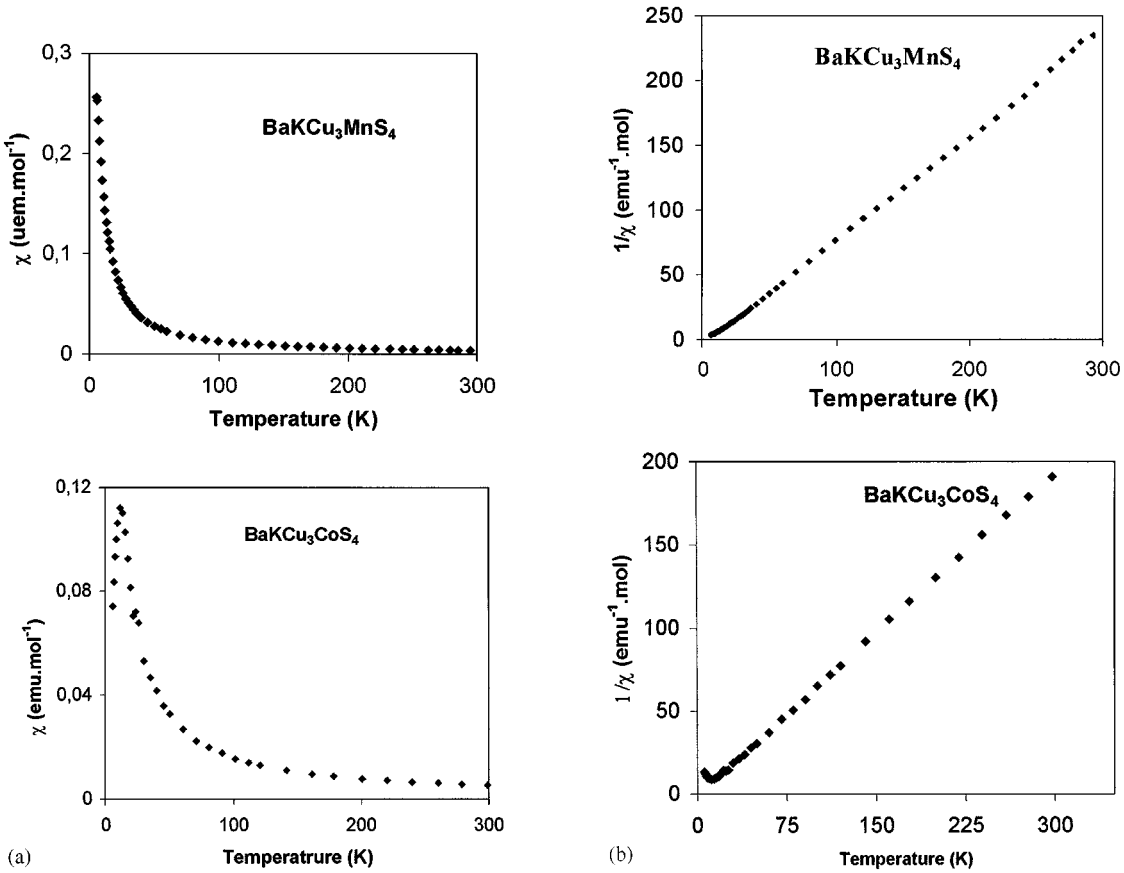

FIG. 3. (a) Magnetic susceptibility as a function of temperature for $BaKCu_3MnS_4$ and $BaKCu_3CoS_4$; (b) inverse magnetic susceptibility.

too large to favor magnetic interactions between manganese ions. On the other hand, $BaKCu_3CoS_4$ exhibits antiferromagnetic interactions below ~ 12 K. Low-temperature FC and ZFC data suggest spin–glass properties owing to Cu–Co disorder (13). The linear plot of χ^{-1} vs T above ~ 50 K yields an effective moment of 2.30 μ_B and a positive Curie–Weiss temperature $\theta = 10$ K (Table 4) consistent with the magnetic properties of the related antiferromagnetic $TlCo_2Se_2$ phase (14, 15). The magnetic moments of $BaKCu_3MnS_4$ and $BaKCu_3CoS_4$ are smaller than expected for free Mn^{2+} and Co^{2+}, 5.92 and 3.87 μ_B, respectively (16). As suggested previously, spin transfer occurring from the 3*p* band of sulfur to the 3*d* band of the transition metal might account for the small μ_{eff} values observed, since spin transfer leads to complete filling of the 3*d* shell of the transition element (17–21). The origin of the suppressed moments may also be due to crystal field effects associated with the short *M*–*M* contacts as described by Bronger *et al.* in many related sulfides (22–24).

In contrast to $BaKCu_3MnS_4$ and $BaKCu_3CoS_4$, a temperature-independent component dominates the susceptibility behavior of the nickel analogue down to 30 K ($\chi_{TIP} = 126 \times 10^{-5}$ emu.mol^{-1}) (Fig. 4). This result shows that the Ni ion does not have localized magnetic moment in $BaKCu_3NiS_4$, as observed in the structurally related chalcogenides KNi_2X_2 (X = S, Se) (14). The low-temperature upturn is most likely due to the presence of paramagnetic impurities in the sample.

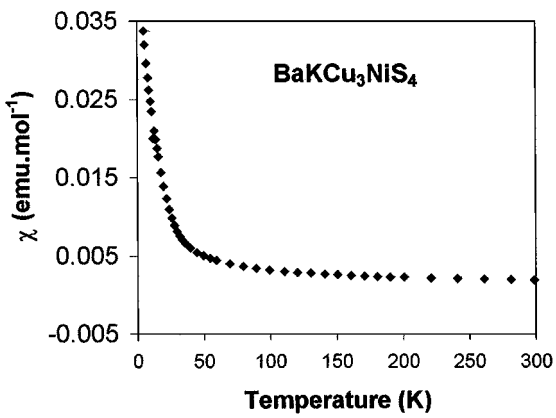

FIG. 4. Temperature dependence of the magnetic susceptibility for $BaKCu_3NiS_4$.

TABLE 4
Magnetic Properties of Transition Metal Sulfides $BaKCu_3MS_4$ (M = Mn, Co, Ni)[a]

Compound	χ_{RT} (emu.mol^{-1})	μ_{eff} (μ_B)	θ (K)
$BaKCu_3MnS_4$	4.256×10^{-3}	2.50	2
$BaKCu_3CoS_4$	4.463×10^{-3}	2.30	10
$BaKCu_3NiS_4$	6.287×10^{-4}	—	—

[a] χ_{TIP} (Ni) = 126×10^{-5} emu.mol^{-1}.

4. CONCLUSION

Single-phase polycrystalline sulfides $BaKCu_3MS_4$ (M = Mn, Co, Ni) were prepared for the first time by CS_2/N_2 sulfurization of $BaCO_3$, K_2CO_3, and the corresponding transition metal oxides. Electrical resistivity measurements show that the replacement of half of the copper ions in $Ba_{0.80}K_{0.20}Cu_2S_2$ by some divalent element Mn^{2+}, Co^{2+}, Ni^{2+} along with an enhancement of the Ba^{2+}substitution for K^+ drastically changes the electric properties from metallic $Ba_{0.80}K_{0.20}Cu_2S_2$ to semiconducting $BaKCu_3MS_4$ materials. Furthermore, the magnetic properties of those compounds depend on the substituting element. Indeed, $BaKCu_3MnS_4$ exhibits Curie-like behavior while the temperature dependence of the magnetic susceptibility of the cobalt analogue shows a maximum which was attributed to short-range antiferromagnetic interactions. Besides, a temperature-independent paramagnetic component dominates the susceptibility behavior of $BaKCu_3NiS_4$.

REFERENCES

1. T. H. Geballe, *Science* **259,** 1550 (1993).
2. C. H. W. Jones, P. E. Kovacs, R. D. Sharma, and R. S. McMillan, *J. Phys. Chem.* **94,** 832(1990).
3. R. Fong, J. R. Dahn, R. J. Batchelor, F. W. B. Einstein, and C. H. W. Jones, *Phys. Rev. B* **39,** 4424 (1989).
4. Z. Ban and M. Sikirica, *Acta Crystallogr.* **18,** 594 (1965).
5. M. Mouallem-Bahout, O. Peña, C. Carel, A. Ouammou, and E.-H. Aqachmar, *Ann. Chim. Fr.* (2000), in press.
6. M. Mouallem-Bahout, O. Peña, C. Carel, A. Ouammou, and M. Retat-Savel'eva, *Zh. Neorg. Khim.* (2000), in press.
7. A. Ouammou, M. Mouallem-Bahout, J.-F. Halet, J.-Y. Saillard, and C. Carel, *J. Solid State Chem.* **117,** 73 (1995).
8. M. Mouallem-Bahout, M. Potel, J.-F. Halet, M. Retat-Savel'eva, J. Padiou, and C. Carel, *Eur. J. Solid State Inorg. Chem.* **33,** 483 (1996).
9. G. Brun, B. Gardes, J.-C. Tedenac, A. Raymond, and M. Maurin, *Mater. Res. Soc. Bull.* **14,** 743 (1979).
10. R. Berger and C. F. van Bruggen, *J. Less-Common Met.* **99,** 113 (1984).
11. J. Llanos, P. Valenzuela, C. Mujica, and A. Buljan, *J. Solid State Chem.* **122,** 31 (1996).
12. M. Oledzka, C. L. Lee, K. V. Ramanujachary, and M. Greenblatt, *Mater. Res. Soc. Bull.* **32,** 889 (1997).
13. M. Mouallem-Bahout, O. Peña, A. Ouammou, and Carel, *J. Phys. Chem. Solids* (2000), in press.
14. G. Huan, M. Greenblatt, and M. Croft, *Eur. J. Solid State Inorg. Chem.* **26,** 193 (1989).
15. M. Oledzka, J. G. Lee, K. V. Ramanujachary, and M. Greenblatt, *J. Solid State Chem.* **127,** 151 (1996).
16. C. Kittel, *in* "Introduction to Solid State Physics" (J. H. Hollomon, Ed.). Wiley, New York, 1965.
17. I. Felner, I. Mayer, A. Grill, and M. M. Schieber, *Solid State Commun.* **16,** 1005 (1975).
18. S. Siek, A. Szytula, and J. Leciejewicz, *Solid State Commun.* **39,** 863 (1981).
19. J. Leciejewicz, M. Kolenda, and A. Szytula, *Solid State Commun.* **45,** 145 (1983).
20. A. Szytula, J. Leciejewicz, and H. Binczycka, *Phys. Stat. Sol. A* **58,** 67 (1980).
21. W. M. McCall, K. S. V. L. Narasiham, and R. A. Butera, *J. Appl. Phys.* **44,** 4724 (1973).
22. I. Felner, *J. Phys. Chem. Solids* **36,** 1063 (1975).
23. W. Bronger, *in* "Crystallography and Crystal Chemistry of Materials with Layered Structures" (F. Levy, Ed.), pp. 93–125. Reidel, Dordrecht, 1976.
24. W. Bronger, H. Hardtdegen, M. Kanert, P. Müller, and D. Schmitz, *Z. Anorg. Allg. Chem.* **662,** 313 (1996).
25. D. Schmitz and W. Bronger, *Z. Anorg. Allg. Chem.* **248,** 248 (1987).